Research Article | Vol. 25, No. 26 | 25 Dec 2017 | OPTICS EXPRESS 32792
Optics EXPRESS

Role of interactions in the magneto-plasmonic response at the geometrical threshold of surface continuity

Evangelos Th. Papaioannou,[1,*] Hui Fang,[2] Blanca Caballero,[3] Eser Metin Akinoglu,[2,4] Michael Giersig,[2,5] Antonio García-Martín,[3] and Paul Fumagalli[2,6]

[1] *Fachbereich Physik and Landesforschungszentrum OPTIMAS, Technische Universität Kaiserslautern, Erwin-Schrödinger-Str. 56, 67663 Kaiserslautern, Germany*
[2] *Institut für Experimentalphysik, Freie Universität Berlin, 14195 Berlin, Germany*
[3] *IMM-Instituto de Microelectronica de Madrid (CNM-CSIC), Isaac Newton 8, PTM, Tres Cantos, E-28760 Madrid, Spain*
[4] *South China Normal University, International Academy of Optoelectronics at Zhaoqing, Zhaoqing, Guangdong, China*
[5] *Helmholtz Zentrum Berlin, Institute of Nanoarchitectures for Energy Conversion, 14195 Berlin, Germany*
[6] *paul.fumagalli@fu-berlin.de*
[*] *papaio@rhrk.uni-kl.de*

Abstract: The optical and magneto-optical behavior in periodically nanostructured surfaces at the threshold of surface continuity is revealed. We address Co films that evolve from an island-like array to a connecting network of islands that form a membrane pattern. The analysis of magneto-optical spectra as well as numerical simulations show significant differences between continuous and broken membranes that depend dramatically on the energy of the incoming radiation. Light localization increases the magneto-optical signal in the membranes. However, the generation of hot spots is not accompanied with magneto-optic enhancement. The electromagnetic field profile within the membrane system can explain the differences in the transmission and in the magneto-optic Kerr signal.

OCIS codes: (160.3820) Magneto-optical materials; (310.6628) Subwavelength structures, nanostructures; (240.6680) Surface plasmons

References and links

1. G. Armelles, A. Cebollada, A. García-Martín, and M. U. Gonzalez, "Magnetoplasmonics: Combining magnetic and plasmonic functionalities," Adv. Opt. Mater. **1**, 10–35 (2013).
2. I. S. Maksymov, "Magneto-plasmonics and resonant interaction of light with dynamic magnetisation in metallic and all-magneto-dielectric nanostructures," Nanomaterials **5**, 577–613 (2015).
3. D. Bossini, V. I. Belotelov, A. K. Zvezdin, A. N. Kalish, and A. V. Kimel, "Magnetoplasmonics and femtosecond optomagnetism at the nanoscale," ACS Photonics **3**, 1385–1400 (2016).
4. M. Rollinger, P. Thielen, E. Melander, E. Östman, V. Kapaklis, B. Obry, M. Cinchetti, A. García-Martín, M. Aeschlimann, and E. T. Papaioannou, "Light localization and magneto-optic enhancement in Ni antidot arrays," Nano Lett. **16**, 2432–2438 (2016).
5. H. Fang, B. Caballero, E. M. Akinoglu, E. T. Papaioannou, A. García-Martín, J. C. Cuevas, M. Giersig, and P. Fumagalli, "Observation of a hole-size-dependent energy shift of the surface-plasmon resonance in Ni antidot thin films," Appl. Phys. Lett. **106**, 153104 (2015).
6. E. Melander, E. Östman, J. Keller, J. Schmidt, E. T. Papaioannou, V. Kapaklis, U. B. Arnalds, B. Caballero, A. García-Martín, J. C. Cuevas, and B. Hjörvarsson, "Influence of the magnetic field on the plasmonic properties of transparent Ni anti-dot arrays," Appl. Phys. Lett. **101**, 063107 (2012).
7. N. Maccaferri, A. Berger, S. Bonetti, V. Bonanni, M. Kataja, Q. H. Qin, S. van Dijken, Z. Pirzadeh, A. Dmitriev, J. Nogu?s, J. Åkerman, and P. Vavassori, "Surface lattice resonances and magneto-optical response in magnetic nanoparticle arrays," Phys. Rev. Lett. **111**, 167401 (2013).
8. M. Kataja, T. K. Hakala, A. Julku, M. J. Huttunen, S. van Dijken, and P. Torma, "Surface lattice resonances and magneto-optical response in magnetic nanoparticle arrays," Nat. Commun. **6**, 7072 1–7 (2015).
9. M. Inoue, M. Levy, and A. V. Baryshev, *Magnetophotonics from Theory to Applications* (Springer-Verlag, 2013).
10. I. S. Maksymov, "Magneto-plasmonic nanoantennas: Basics and applications," Rev. Phys. **1**, 36 – 51 (2016).

#304592 https://doi.org/10.1364/OE.25.032792
Journal © 2018 Received 21 Aug 2017; revised 23 Oct 2017; accepted 16 Nov 2017; published 18 Dec 2017
Corrected: 03 January 2018

Optics EXPRESS

11. C.-H. Lambert, S. Mangin, B. S. D. C. S. Varaprasad, Y. K. Takahashi, M. Hehn, M. Cinchetti, G. Malinowski, K. Hono, Y. Fainman, M. Aeschlimann, and E. E. Fullerton, "All-optical control of ferromagnetic thin films and nanostructures," Science **345**, 1337–1340 (2014).
12. V. V. Kruglyak, S. O. Demokritov, and D. Grundler, "Magnonics," J. Phys. D: Appl. Phys. **43**, 264001 (2010).
13. B. Lenk, H. Ulrichs, F. Garbs, and M. M?nzenberg, "The building blocks of magnonics," Phys. Rep. **507**, 107 – 136 (2011).
14. A. V. Chumak, V. I. Vasyuchka, A. A. Serga, and B. Hillebrands, "Magnon spintronics," Nat. Phys. **11**, 453 (2015).
15. K. Uchida, H. Adachi, D. Kikuchi, S. Ito, Z. Qiu, S. Maekawa, and E. Saitoh, "Generation of spin currents by surface plasmon resonance," Nat. Commun. **6**, 5910 (2015).
16. D. Stauffer and A. Aharony, *Introduction to Percolation Theory* (Taylor & Francis Ltd, 1994).
17. K. Kempa, "Percolation effects in the checkerboard babinet series of metamaterial structures," Phys. Status Solidi RRL **4**, 218–220 (2010).
18. Y. Peng, T. Paudel, W.-C. Chen, W. J. Padilla, Z. F. Ren, and K. Kempa, "Percolation and polaritonic effects in periodic planar nanostructures evolving from holes to islands," Appl. Phys. Lett. **97**, 041901 (2010).
19. E. M. Akinoglu, T. Sun, J. Gao, M. Giersig, Z. Ren, and K. Kempa, "Evidence for critical scaling of plasmonic modes at the percolation threshold in metallic nanostructures," Appl. Phys. Lett. **103**, 171106 (2013).
20. E. T. Papaioannou, V. Kapaklis, P. Patoka, M. Giersig, P. Fumagalli, A. García-Martín, E. Ferreiro-Vila, and G. Ctistis, "Magneto-optic enhancement and magnetic properties in Fe antidot films with hexagonal symmetry," Phys. Rev. B **81**, 054424 (2010).
21. E. M. Akinoglu, A. J. Morfa, and M. Giersig, "Nanosphere lithography-exploiting self-assembly on the nanoscale for sophisticated nanostructure fabrication," Turk J Phys. **38 (3)**, 563–572 (2014).
22. E. M. Akinoglu, A. J. Morfa, and M. Giersig, "Understanding anisotropic plasma etching of two-dimensional polystyrene opals for advanced materials fabrication," Langmuir **30**, 12354–12361 (2014).
23. F. Gallego-Gómez, A. Blanco, and C. López, "In situ optical study of water sorption in silica colloidal crystals," J. Phys. Chem. C **116**, 18222–18229 (2012).
24. A. Blanco, F. Gallego-Gómez, and C. López, "Nanoscale morphology of water in silica colloidal crystals," J. Phys. Chem. Lett. **4**, 1136–1142 (2013).
25. C. Genet and T. W. Ebbesen, "Light in tiny holes," Nature **445**, 39–46 (2007).
26. T. W. Ebbesen, H. J. Lezec, H. F. Ghaemi, T. Thio, and P. A. Wolff, "Extraordinary optical transmission through sub-wavelength hole arrays," Nature **391**, 667–669 (1998).
27. N. Maccaferri, X. Inchausti, A. García-Martín, J. C. Cuevas, D. Tripathy, A. O. Adeyeye, and P. Vavassori, "Resonant enhancement of magneto-optical activity induced by surface plasmon polariton modes coupling in 2d magnetoplasmonic crystals," ACS Photonics **2**, 1769–1779 (2015).
28. A. García-Martín, G. Armelles, and S. Pereira, "Light transport in photonic crystals composed of magneto-optically active materials," Phys. Rev. B **71**, 205116 (2005).
29. B. Caballero, A. García-Martín, and J. C. Cuevas, "Generalized scattering-matrix approach for magneto-optics in periodically patterned multilayer systems," Phys. Rev. B **85**, 245103 (2012).
30. COMSOL Multiphysics®. Simulations have been performed with an adaptive dense mesh with at least 15 elements per wavelength (or penetration length in the metals) and a further refinement whenever sharp features are present.
31. E. Ferreiro-Vila, J. B. González-Díaz, R. Fermento, M. U. González, A. García-Martín, J. M. García-Martín, A. Cebollada, G. Armelles, D. Meneses-Rodríguez, and E. M. n. Sandoval, "Intertwined magneto-optical and plasmonic effects in ag/co/ag layered structures," Phys. Rev. B **80**, 125132 (2009).
32. G. Armelles, A. Cebollada, F. Garcí?a, A. García-Martín, and N. de Sousa, "Far- and near-field broad-band magneto-optical functionalities using magnetoplasmonic nanorods," ACS Photonics **3**, 2427–2433 (2016).
33. G. Armelles, B. Caballero, A. Cebollada, A. Garcia-Martin, and D. Meneses-Rodríguez, "Magnetic field modification of optical magnetic dipoles," Nano Lett. **15**, 2045–2049 (2015).
34. J. C. Banth?, D. Meneses-Rodr?guez, F. Garc?a, M. U. Gonz?lez, A. Garc?a-Mart?n, A. Cebollada, and G. Armelles, "High magneto-optical activity and low optical losses in metal-dielectric Au/Co/Au/SiO_2 magnetoplasmonic nanodisks," Adv. Mater. **24**, 36–41 (2012).
35. D. Meneses-Rodríguez, E. Ferreiro-Vila, P. Prieto, J. Anguita, M. U. González, J. M. García-Martín, A. Cebollada, A. García-Martín, and G. Armelles, "Probing the electromagnetic field distribution within a metallic nanodisk," Small **7**, 3317–3323 (2011).
36. B. Caballero, A. García-Martín, and J. C. Cuevas, "Faraday effect in hybrid magneto-plasmonic photonic crystals," Opt. Express **23**, 22238–22249 (2015).

1. Introduction

Patterned ferromagnetic/plasmonic metal films can exhibit strong plasmonic and magneto-plasmonic activity resulting in large enhancement of magneto-optical effects in the presence of localized or propagating surface plasmons [1–3]. Recently, the magneto-plasmonic research has also investigated to what extent pure ferromagnetic patterned films [4–6] and nanoparticles [7, 8]

Optics EXPRESS

can host surface plasmons and increase the magneto-optic response. The technological perspectives of magneto-plasmonic structures are large: the potential capability to trap light locally (near field enhancement) in magneto-plasmonic nanostructures [4, 9, 10] opens new routes in the research of magnetism, optomagnetism and ultrafast all-optical switching [3, 11]. In addition, investigations of plasmon-induced spin wave excitations in magnetic systems can extend the field of magneto-plasmonics research to magnonics [12–14] and spintronics [15].

In this work we focus on the magneto-plasmonic response of pure ferromagnetic films around the geometrical threshold, i.e. the formation of magnetic clusters that can physically touch each other. Particularly, we address periodically nano-perforated cobalt films: films evolving from an island-like array to a connecting network forming an anti-dot pattern. The geometrical transition also defines the plasmonic transition from propagating to localized modes and thus is expected to strongly influence the magneto-optic response. The plasmonic properties of such transition structures can be interpreted with the concept of percolation theory. Percolation theory describes the transition of isolated particles or clusters usually located inside a host matrix, to a kind of a connected network [16]. The rise of nanotechnology has facilitated the preparation of composite multicomponent materials in physics, chemistry and materials science and therefore, it has offered to percolation theory many fields of applications. The physical properties of such structures like electrical and thermal conduction are very interesting since around the percolation threshold a system can behave either as a dielectric or as a conducting medium. This behaviour can also be reflected in the optical properties: in a dielectric-metal transition the change from a positive real part of the dielectric function $\epsilon(\omega)$ for the dielectric to a negative real part of $\epsilon(\omega)$ of the metal will drastically change the optical properties.

The studies on the optical properties on similar hole-to-island structural evolution patterns have shown that the lack of continuity affects the system in a non-trivial way, that may induce not only continuous shifts [5] but also changes on the overall spectral shape of the optical response [17]. Those cases have been qualitatively explained by considering an effective dielectric tensor [18]. Furthermore, a critical behavior of the effective dielectric function was revealed demonstrating that the hole-to-island structural evolution is a topological analog of the percolation threshold at the transitional pattern. In addition, the critical scaling of the plasmonic modes in similar metallic nanonstructures has been discussed [17, 19]. Here we show the effect of surface plasmon resonance on the magneto-optical Kerr effect with respect to the transition from islands (dots) to mebranes (anti-dots) nanostructures composed of thin cobalt layers.

2. Results and discussion

2.1. Sample preparation

All nanostructures were obtained using lithography by self-assembly of colloidal nanospheres. [20, 21] Polystyrene nanospheres with a diameter of $a = 470$ nm have been deposited under appropriate conditions on 0.5 mm thick quartz subtrates. Self-assembly leads to the formation of a hexagonal closed-packed array of nanospheres. Plasma etching was subsequently used in order to shrink the diameter of the spheres [6, 22]. By varying the etching time it was possible to vary d from $d = a = 470$ nm to $d = 300$ nm. A 50 nm Co film was subsequently deposited over each colloidal mask. The last stage of preparation involved cleaning with toluene to remove the polystyrene mask. Figure 1 shows scanning electron microscopy (SEM) images of the resulting Co nanostructures. Since no protective overlayer was deposited, the Co layers can be oxidized at the surface as it can be seen in Fig. 1: the different color at the rim of the holes for the samples with $d = 300, 373$ nm for example, indicate the presence of a self passivating cobalt oxide rather than metallic cobalt. We have measured directly after the preparation of the sample in order to minimize the effect of oxidation.

The samples with $d = 373$ nm and $d = 300$ nm represent a continuous coverage while the rest exhibit an island-like pattern. The given hole diameters in samples with non-continuous coverage

Optics EXPRESS

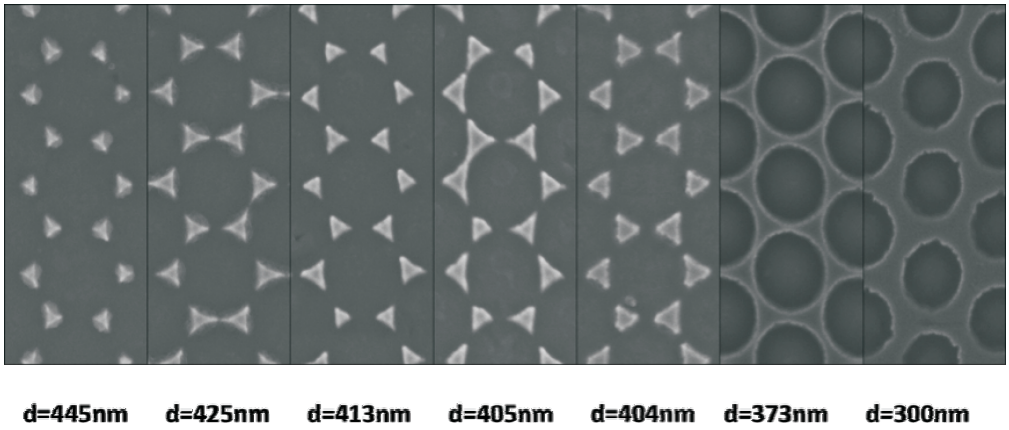

Fig. 1. Scanning electron microscopy images for seven different Co films deposited on quartz substrates. The center to center distance is $a = 470$ nm. Only two samples with $d = 373$ nm and $d = 300$ nm present a continuous coverage. The rest of the samples have an island like shape. The percolation limit between isolated islands and connected islands lies around d values of $d = 425, 413, 405$ and 373 nm.

have been calculated from the etching time and verified by the SEM images. It is important to notice that all samples should be membranes with continuous Co coverage, since all diameters are smaller than the lattice parameter. The non-continuity is induced during the deposition process. The high directionality of the evaporation beam leads to the formation of bridges between the spheres [23, 24] and facilitates our purposes to create structures around the percolation limit.

2.2. Optical and magneto-optical characterization

Figure 2(a) presents the experimental transmission spectra for the nanostructures presented in Fig. 1. The overall transmission decreases as the hole diameter decreases. This can be attributed to the increasing Co coverage as the diameter of the holes decreases. However, the spectra present qualitatively different features that require further attention. From the spectrum corresponding to sample with $d = 300$ nm, the one with more Co coverage (membrane like), we can see the typical features encountered in systems exhibiting extraordinary transmission: two well pronounced transmission maxima, and two transmission minima whose spectral position correspond to that expected from Bragg orders [25].

These transmission features are related to the periodicity of the pattern, and should not change position as a function of the holes diameter except for the small effects that the polydispersity of the nanospheres produce. It is indeed seen that the features remain, but are washed out as the Co amount decreases. The maxima between the Bragg features observed in $d = 300$ nm are the typical manifestation of extraordinary optical transmission in metallic samples, and have been associated to the excitation of Bragg-plasmons, i.e. lattice modes with a plasmonic character [6, 26, 27]. These maxima change position as the plasmon characteristics change when the holes diameter increases [5]. But for the rest of the samples there is an overall shape modification especially for the low energy part of the spectrum. This sudden change is evolving near the percolation limit since it is related to the disruption of the continuity of the cobalt over the quartz substrate.

To shed light into the experimental findings we have performed numerical simulations using both scattering matrix approaches [28, 29] and Finite Element [30] of connected and disconnected networks with the same nominal hole diameters. The purpose is to establish if there is a qualitative

Optics EXPRESS

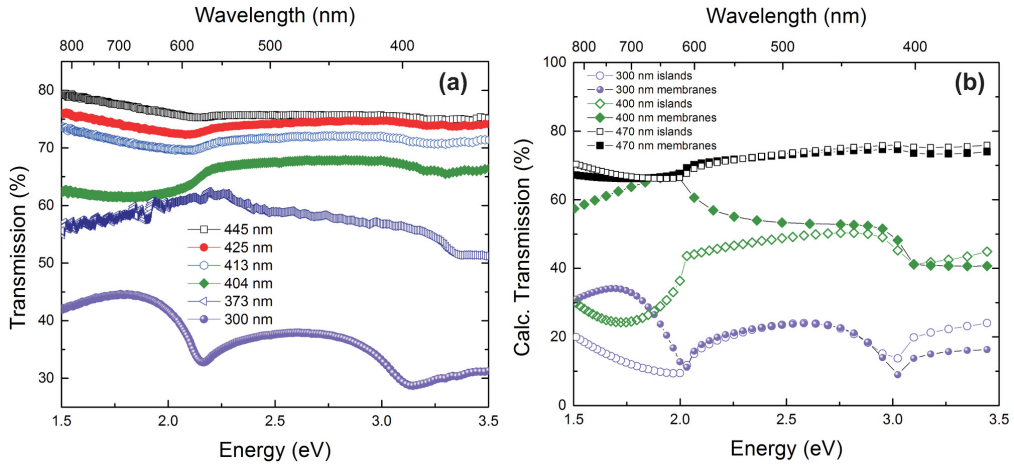

Fig. 2. (a) Experimental transmission spectra for the Co nanostructured thin films with different hole diameters. Clear extraordinary transmission peaks are observed for the continuous structure with d = 300 nm while there is gradually change of the shape of the spectra at the percolation limit. (b) Calculated transmission spectra for Co nanostructured thin films with different hole diameters as indicated. Filled symbols are for continuous membranes, and the open symbols are for the same structure but with a 60 nm gap breaking the bridges, resembling in such a way the islands.

difference in the spectra due to the metal continuity. Transmission spectra are presented in Fig. 2(b) for membranes (filled symbols) with different hole diameters but keeping the same lattice parameter a = 470 nm, together with spectra corresponding to the very same structures, but with the metallic bridges broken by a 60 nm gap to mimic the discontinuity of the actual samples (open symbols). It has to be noted that the same gap size is used for all the simulated structures. The first apparent effect of the metal discontinuity can be seen in a marked difference in the low-energy part of the spectra, while the difference is smaller, if any, in the high-energy part. We will see, through calculations of the spatial distribution of the electromagnetic field, that the dissimilarity between the low-energy and high-energy part can be understood by light scattering in the broken regions and the generation of optical hot-spots.

In the low energy region, the spectral behaviour for continuous and broken membranes is different, not only quantitatively but also qualitatively. Maxima associated with the extraordinary transmission phenomena are present for unbroken membranes. In addition, the maxima are blue-shifted as the diameter of the hole increases in a similar way as in [5]. However, for broken membranes, the behaviour is the opposite. Minima appear which are red-shifted when the diameter of the holes increases. Both (maxima and minima) exhibit a sharp feature when the resonance spectrally overlaps with the lattice resonance. The high energy regions of the two systems exhibit a more similar behavior, presenting quantitative differences. The case of touching spheres, d = 470 nm, gives the same result with and without the presence of the gap.

Of great interest is the comparison for the samples around the geometrical transition: the theoretical curve for the continuous membrane with d = 400 nm presents an equivalent shape to that of the sample with d = 373 nm (experiment) pointing to the fact that the experimental sample is still continuous. In this case the plasmonic resonance and the Wood anomaly are close enough to alter the shape from a rounded peak to a maximum with a sharp structure (as seen in both experiment and theory). In short, the distinct feature is a maximum in transmission for continuous membranes and a minimum for the islands (see for example the region from 1. 5 eV

Optics EXPRESS

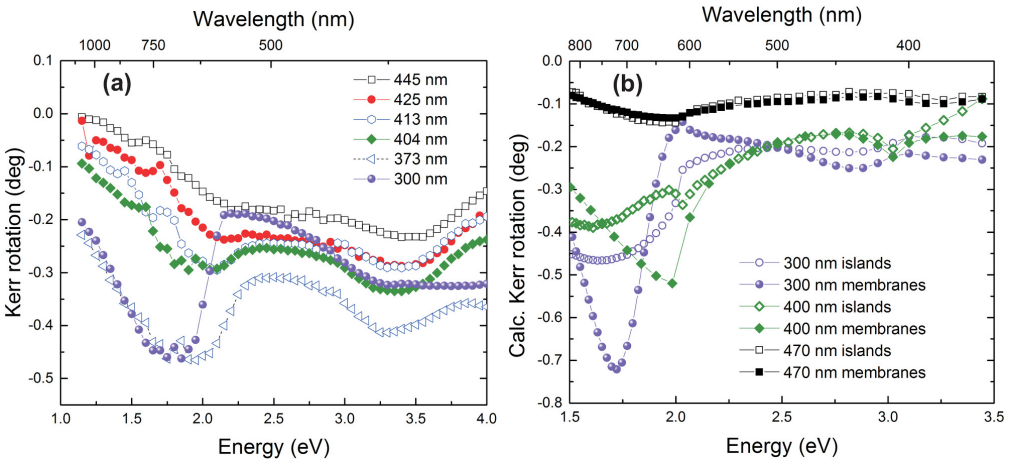

Fig. 3. (a) Experimental polar Kerr rotation spectra for islands and membranes of diameter size from $d = 300$ to 445 nm. The Kerr rotation increases with decreasing the hole diameter. Opposite to the sharp changes in the transmission curves the Kerr spectra exhibit a more similar shape for both broken and unbroken membranes. (b) Simulated polar Kerr rotation versus photon energy for islands and membranes of diameter size $d = 300, 400, 470$ nm. Filled symbols refer to continuous membranes, and the open symbols correspond to the same structure but with a 60 nm gap breaking the bridges similar to Fig.2(b).

to 2 eV).

To summarize the optical characterization, the transmission curves exhibit different shapes at the percolation limit. The more pronounced difference appears at low frequencies. The extraordinary transmission peaks due to the coupling of the incident light to the surface plasmons though the lattice for the continuous membranes are replaced with minima in transmission for the broken island-type structures. The results of the numerical simulations fully agree with the experimental data in terms of the shape of the curves, revealing after all that the physics of the experiment is well captured by the theory. However, there are small deviations in the calculated intensities and the spectral position of the curve features. Multiple factors are behind these deviations. The most important one is the accuracy of the material parameters. We have used for our simulations the experimentally obtained values for Co from [31], but the fabrication process (grain size, humidity, temperature, etc.) affects the outcome. The oxidation of the Co layer is another major factor since in the simulations the optical and magneto-optical constants obtained from a pristine Co film were considered. The oxidation in our case leads to a shift of the experiment curves similarly to other published works, not only for Co, but other ferromagnetic metals [6, 32–34]. Besides that, the intensity will be also influenced by the surface oxidation. In the experiment, we observe higher transmission due to the fact that the oxidation reduces the metallic character of the films. Geometrical inhomogeneities of the pattern can also affect the comparison.

In Fig. 3(a) we present the experimental Kerr rotation spectra for the same samples as in Fig. 2(a). As one can readily see, the overall trend is that the Kerr rotation increases (the sign only reflects the direction of the Kerr rotation) with decreasing the hole diameter, as the amount of Co increases. However, the spectra present two main features for energies matching those appearing in the transmission spectra. In contrast to the sharp, qualitative change in the spectral shape found in the optical spectra for the broken and unbroken case, the Kerr spectra exhibit a more similar shape, with minima and maxima around the same positions (except for small

Optics EXPRESS

spectral shifts). Quantitively, the maximum value of the Kerr rotation is seen for the cases of $d = 300, 373$ nm, more pronounced in the low energy region where the transmission curves exhibit large amplitude changes. The second maximum at the high energy region $\approx 3.2 - 3.3$ eV is present for all samples being more pronounced for the $d = 373$ nm sample.

In order to complement our experimental observations, we have performed calculations of the polar Kerr rotation spectra for the same geometrical parameters as for the optical analysis in Fig. 2(b). The data for Co used here were taken from [31] where the optical and magneto-optical constants of Co were experimentally determined, through a combination of ellipsometry and polar Kerr and Kerr ellipticity measurements. Dispersion, i.e. wavelength dependence, of the material parameters and the gyration of Co was taken into account. As shown in Fig. 3(b), the calculated Kerr rotation spectra indicate the same trend as the experimental data, pointing out that there is not a clear qualitative difference for broken and unbroken membranes. It is also evident that the sample with a hole diameter of $d = 470$ nm exhibits no difference at all. The samples $d = 300$ and 400 nm membranes in Fig. 3(b), are closely related to the transmission of the experimental antidot structures of $d = 300$ and $d = 373$ in Fig. 2(a). Generally, there is a quantitative modification of the Kerr rotation in the low energy region, but the features are similar in shape (minima stay minima irrespective of the state of the membrane), they stay in the same energy location and the spectra follow the (overall) trend: the smaller the hole the larger the Kerr rotation, due to the larger amount of Co in the system.

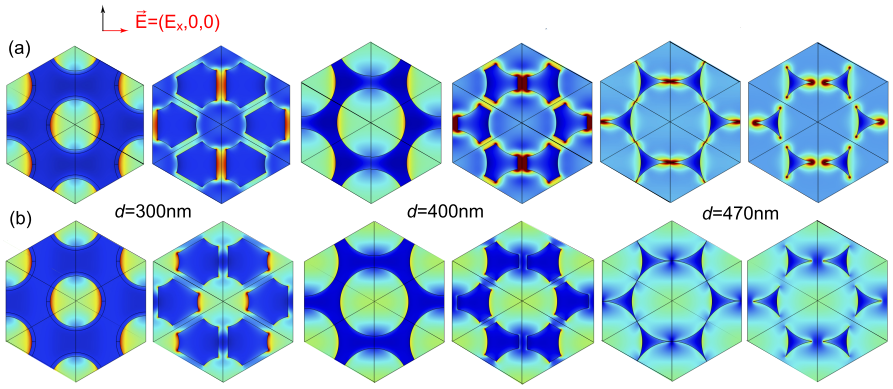

Fig. 4. Calculated intensity of the electric field $|E^2|$ 10nm below the upper surface for unbroken (u) and for broken (b) membranes, for hole diameter sizes of $d = 300, 400, 470$ nm. (a) Low energy spectral region, where the incoming plane wave has an energy of 1.7 eV. Clear differences between unbroken and broken membranes can be clearly seen. (b) High energy spectral region (2.7 eV), where differences are actually very small.

In order to reveal the origin of the differences found in the transmission and polar Kerr spectra, we will analyze an important factor in these kind of systems: the spatial distribution of the electromagnetic field in the structure. The localisation of the electromagnetic field is a key parameter that can define the optical response and the magneto-optical enhancement in metallic systems [4, 35, 36]. In Fig. 4 we present the spatial profile of the electromagnetic field distribution in a plane located 10 nm below the top surface of the membrane obtained for two energies that correspond to the locations of the maxima in transmission. In Fig. 4 (a) the profiles correspond to an incoming wave with an energy of 1.7 eV corresponding to the low energy region, whereas in Fig. 4(b) the energy is 2.7 eV and is located in the high energy range. In the case of the low energy range, and for $d = 300, 400$ nm hole diameters, there is a field enhancement in the direction parallel to the polarization axis (E_x) and the field localization occurs in the holes.

Optics EXPRESS

However, for the broken membranes the spatial location varies, the field localization happens in the gaps that are perpendicular to the the polarization direction. In addition, the field in the holes (non-absorbing part of the membrane) decreases for broken geometries. The field within the metal presents differences but not as dramatic as for the holes. For the $d = 470$ nm sample the profiles are very similar. The bridges are so thin that the penetration in the metal (up to the skin depth $\sim 5 - 8$ nm) is enough to give rise to hot spots in the unbroken membranes similar to the broken ones. The presence of these hot spots contributes to an effective decrease of the field that would travel through the membrane and thus eventually accounts for the transmission.

The results of Fig. 3 have revealed a more quantitative than qualitative difference (shape) in the Kerr spectra between membranes and islands. The differences can be understood with the help of Fig. 4: the enhancement of the Kerr signal comes from the intensification of the electromagnetic field that probes the metal for $d = 300, 400$ nm hole diameters. However, the appearance of hot spots in the islands and in the $d = 470$ nm membrane in Fig. 4(a) changes the localization pattern but it does not result in an enhancement of the magneto-optic signal. The situation for the high energy range Fig. 4(b) is completely different: no hot spots are present for any of the geometries, and very subtle differences can be seen for broken and unbroken cases. This is the reason behind the very similar values for both transmission and Kerr rotation in this energy range.

3. Conclusions

The presented set of Co nanostructured thin films were prepared by nanosphere lithography, a method that enabled the fabrication of continuous, anti-dot structures as well as of broken, island-like arrays. The optical and magneto-optical measurements have revealed a qualitative difference in their spectral shape. Numerical simulations show that the effect of 'continuity' is more pronounced in the low energy region of the optical spectra and that is supported by the spatial distribution of the electromagnetic field in the membrane. The formation of hot spots is the reason for the difference in both transmission and Kerr rotation for broken and unbroken systems. For very thin linking bridges the penetration of the field within the metal gives rise to hot spots before the membrane is actually broken and thus no noticeable difference can be seen for broken/unbroken systems.

Funding

Deutsche Forschungsgemeinschaft (DFG) (SFB/TRR 173: SPIN+X, Project B07); Carl Zeiss Foundation; China Scholarship Council (CSC); Spanish Ministry of Economy and Competitiveness (MAT2014-58860-P); Comunidad de Madrid Program (S2013/MIT-2740); Guangdong Innovative and Entrepreneurial Team Program.

Acknowledgments

E.Th.P acknowledges the collaborative research center SFB/TRR 173: SPIN+X: Spin in its collective environment-Project B07 of the Deutsche Forschungsgemeinschaft (DFG), and the Carl Zeiss Foundation. H.F. acknowledges the financial support by the China Scholarship Council (CSC). A.G.-M. and B.C. gratefully acknowledge support by the Spanish Ministry of Economy and Competitiveness through grant MAT2014-58860-P and by the Comunidad de Madrid through Contract No. S2013/MIT-2740. E. M. A. acknowledges the Guangdong Innovative and Entrepreneurial Team Program: Plasmonic Nanomaterials and Quantum Dots for Light Management in Optoelectronic Devices.